

complexity. The availability of the Ferranti Mercury computer with its large storage facilities and high operational speed suggests the design of a programme for carrying out this procedure in which as much work as possible is done inside the machine and machine output is reduced to a minimum.

Work has begun on the design of a programme which will do the following:

- (i) Read in the following data: (a) unit-cell dimensions, (b) the number and relative weights of atoms in the unit cell, (c) all intensities, (d) the symmetry of the unit cell.
- (ii) Calculate the U 's and find all the sign and inequality relationships which inter-relate the largest of them. If the number of relationships is too small compared with the number of U 's then more U 's will be taken until there are about twice as many relationships as unknown signs.

At this stage the fraction of sign relationships expected to hold will be calculated (Cochran & Woolfson, 1955). This should be at least 85% if the method is to be successful.

- (iii) Find all plausible sets of signs for the largest U 's and then derive a number of additional signs for U 's of moderate magnitude by using the relationship

$$s(\mathbf{h}) = s\left(\sum_{\mathbf{h}'} U_{\mathbf{h}'} U_{\mathbf{h}+\mathbf{h}'}\right)$$

(§ 4.4, Cochran & Woolfson, 1955).

- (iv) Apply the Z test to each set of signs and output the best few sets in the form of Fourier syntheses.

Initially a pilot programme will be designed for two-dimensional work only. When this is working satisfactorily, and if the results seem to justify the step, a more ambitious programme to tackle three-dimensional problems will be developed.

The author is indebted to Prof. F. C. Williams, of the Manchester University Computing Machine Laboratory, for the computing facilities which made possible the work described in this paper.

References

- COCHRAN, W. & DOUGLAS, A. S. (1957). *Proc. Roy. Soc. A*, **243**, 281.
 COCHRAN, W. & PENFOLD, B. R. (1952). *Acta Cryst.* **5**, 644.
 COCHRAN, W. & WOOLFSON, M. M. (1955). *Acta Cryst.* **8**, 1.
 McDONALD, T. R. R. & BEEVERS, C. A. (1952). *Acta Cryst.* **5**, 654.
 SAYRE, D. (1951). *Acta Cryst.* **4**, 362.
 SAYRE, D. (1952). *Acta Cryst.* **5**, 60.
 WOOLFSON, M. M. (1957). *Acta Cryst.* **10**, 116.
 WOOLFSON, M. M. (1958). *Acta Cryst.* **11**, 277.

Acta Cryst. (1958). **11**, 397

Surface Melt Patterns on Silicon

By G. L. PEARSON AND R. G. TREUTING

Bell Telephone Laboratories Incorporated, Murray Hill, N. J., U.S.A.

(Received 8 October 1957 and in revised form 10 December 1957)

Surface melt patterns have been formed on silicon by heating to within a few degrees of the melting point (1412° C.), followed by a rapid quench. Localized melting occurs where specks of impurities reside on the surface. Straight-sided geometrical patterns several microns in extent are thus formed, and their shapes are uniquely determined by the surface crystal plane. Conclusive proof that these melt patterns are defined by {111} planes rather than any other system has been obtained through a study of their shapes on rational crystal surfaces presented by multi-twinned crystals. We have formed similar patterns on germanium, indium antimonide, gallium antimonide, and gallium arsenide crystals with this technique.

Introduction

Although thorough studies have been made on the detailed mechanisms of crystal growth, very little has been reported on the converse mechanisms involved in crystal melting. The present paper describes certain geometric patterns formed on the surfaces of silicon

single crystals following the initiation of melting. The shapes of these melt patterns are uniquely determined by the lattice orientation of the face on which they are formed, the contours being the intersections of the close-packed {111} planes with the surface. Nucleation of melting is effected by minute impurities residing on the surface which lower the melting point in their

immediate vicinity, rather than by crystal imperfections.

Following is a collection of physical properties of silicon which will be useful in interpreting some of the results. Silicon crystallizes in the diamond structure. Its lattice constant at 25° C. is 5.431×10^{-8} cm. and the linear thermal expansion coefficient at this temperature is $4.2 \times 10^{-6}/^{\circ}\text{C}$. (Straumanis & Aka, 1952). The melting point is $1412 \pm 2^{\circ}\text{C}$., and there is a decrease in volume of about 9% in passing from the solid to the liquid form (Bond & Logan, 1958). The specific heat of silicon is 6.53 calories/ $^{\circ}\text{C}$./gram-atom below its melting point and 6.12 calories/ $^{\circ}\text{C}$./gram-atom above (Olette, 1957). The latent heat of fusion is 12,095 calories/gram-atom, which is higher than that reported for any other element (Olette, 1957).

Experimental procedure and results

The silicon single crystals used in this study were grown from the melt, and were oriented using X-ray techniques. Long rectangular rods were sawed and ground having low-index planes as lateral faces; in particular these were $\{100\}$, $\{110\}$, $\{111\}$, and $\{211\}$. The rods were then etched in a cp-8 solution (25 cm.³ HNO₃ + 25 cm.³ HF) to obtain a smooth surface. They were next cleaned in an aqueous solution of KCN to remove foreign metal contaminant from their surfaces, and then rinsed in deionized water. After drying, they were heated close to 1415° C. by passing an electric current through them in air. Following cooling by a quick quench in air, they were examined under a microscope and found to have surface melt patterns as shown in the photomicrographs reproduced in Fig. 1. It can be seen that the outer contours of these patterns are uniquely determined by the surface plane on which they are formed, being squares on the $\{100\}$ surface, equilateral triangles on the $\{111\}$ surface, parallel striations on the $\{110\}$ surface, and isosceles triangles on the $\{211\}$ surface.

Although the symmetrical contours of melt patterns on the different surfaces are shown in detail in Fig. 1, the depth of focus in these photomicrographs is too limited to show the vertical details. Fig. 2 is a cross-section drawing of a typical melt pattern on a $\{100\}$ surface, and indicates the hemispherical hill which is

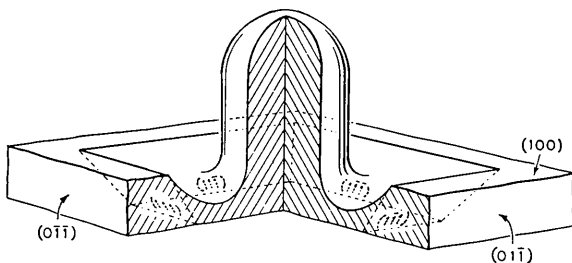


Fig. 2. Perspective drawing of a typical melt pattern on the $\{100\}$ surface of silicon.

present in the center of all such patterns. It is our belief that, following melting, surface tension pulls the contracted molten material to form this hill leaving the surrounding pit, and that the hill then grows in volume during subsequent freezing. It seems probable that atoms attached to the $\{111\}$ close-packed planes should be the most difficult to remove, and it will be shown in the following that the outer contours of the depression are in fact formed by such refractory $\{111\}$ planes intersecting the surface.

Crystallographic analysis

To establish uniquely the crystal plane bounding the pits, traces on surfaces of lower symmetry than those so far described are helpful to the analysis. A suitable specimen was provided by a doubly twinned silicon bar initially grown in a $\langle 111 \rangle$ direction and cut to be bounded by $\{110\}$ and $\{112\}$ prismatic faces. The crystal faces of lower symmetry thus exposed showed differently shaped melt patterns bounded by additional directions of intersection of bounding planes with the surfaces.

The specimen is shown in Fig. 3, with the twin com-

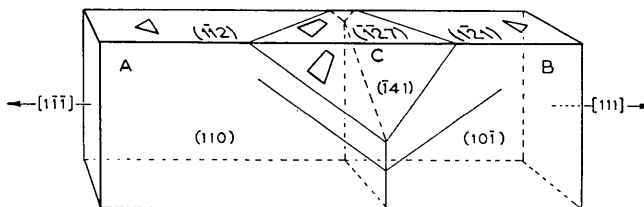


Fig. 3. Silicon bar with twin components *A*, *B*, *C*, and form of melt contours on front and top surfaces.

ponents labeled *A*, *B*, and *C*, and with the contours generated on the front and top surfaces sketched for each component. Fig. 4 shows photomicrographs of the top, front, and bottom surfaces. In each case, the surface melt patterns of all components are included. The mirror relation of the patterns across the *AB* twinning planes is evident. The unsymmetrical, four-sided patterns on the *C* component permit conclusive determination of the form of the bounding plane.

The orientations were obtained with back-reflection Laue X-ray photographs taken on each component and on the *AB*, *BC*, and *CA* boundaries. The orientation relationships and twin composition planes were obtained from stereographic projections and the twin plane surface traces (see, for example, Barrett, 1952). The situation is summarized in the composite projection of Fig. 5. Components *B* and *C* are each a first-order twin of *A*, so that *B* is therefore a second-order twin of *C*. The three orientations have a $\langle 110 \rangle$ pole in common; the indexing is such that this is the $[0\bar{1}1]$ direction in each. The resulting indices of the surfaces and growth directions are shown in Fig. 5 and summarized in Table 1. The stereographic derivation was

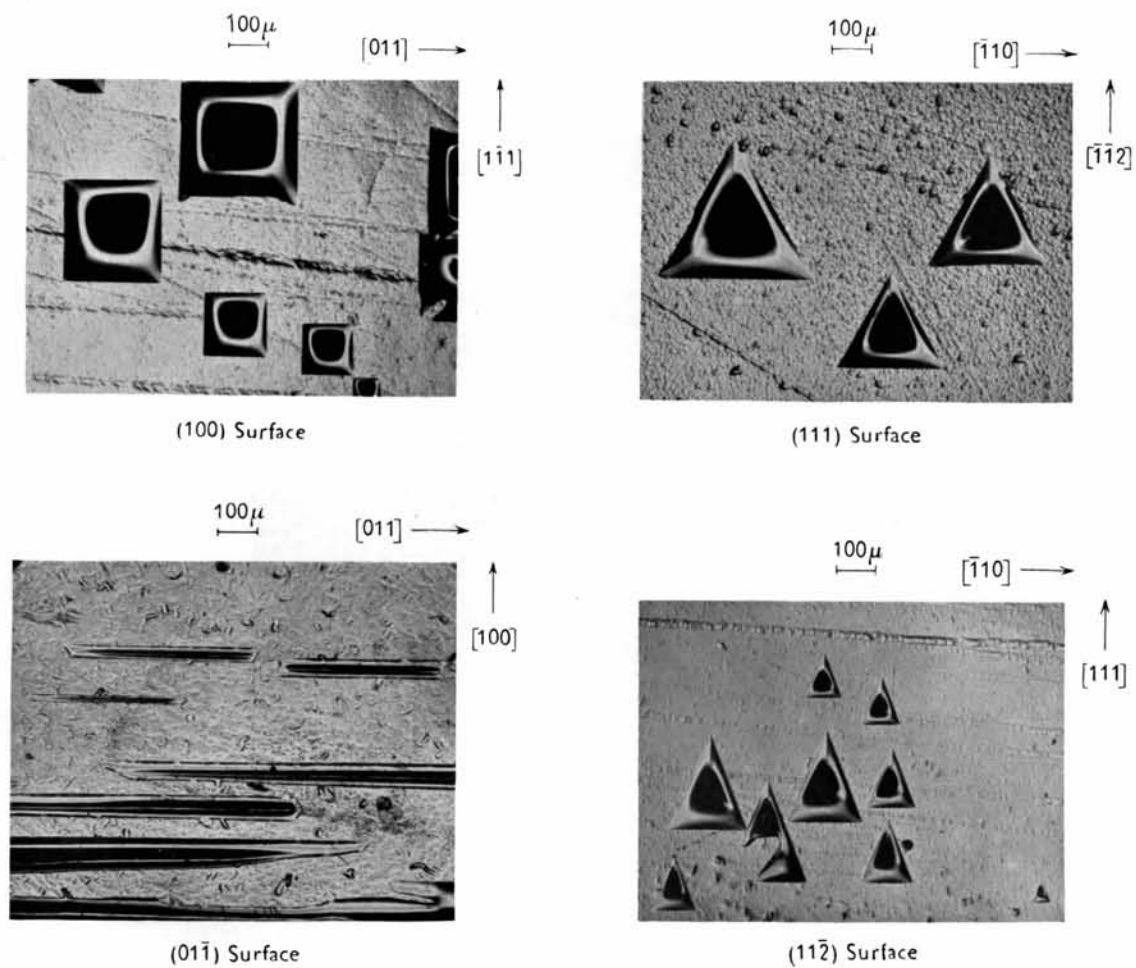


Fig. 1. Photomicrograph of melt patterns on low-index silicon surfaces.

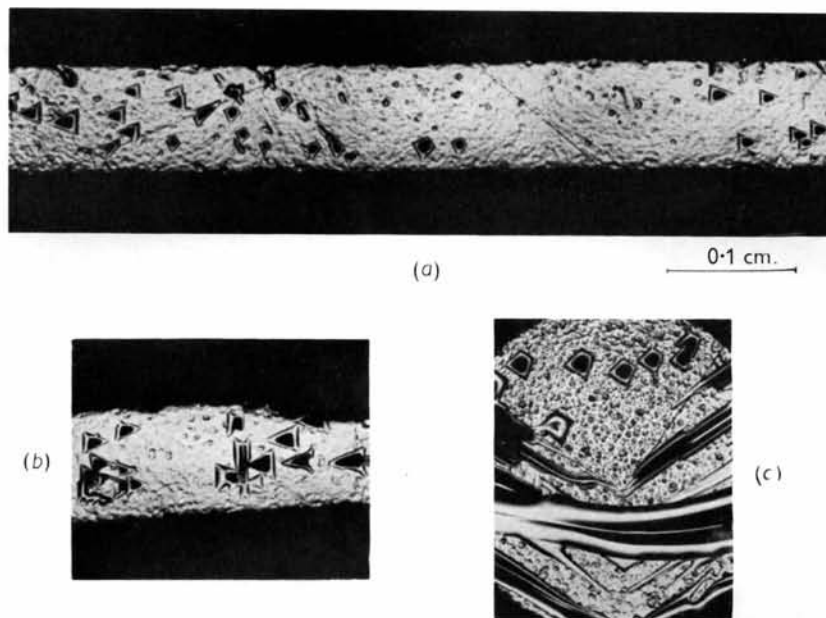


Fig. 4. Photomicrographs of melt patterns on silicon bar of Fig. 3:
 (a) top surface, (b) bottom surface, (c) front surface.

confirmed analytically following general transformation methods given by Bond (1946, 1948). It is shown from the traces in Fig. 5 that the BC boundary con-

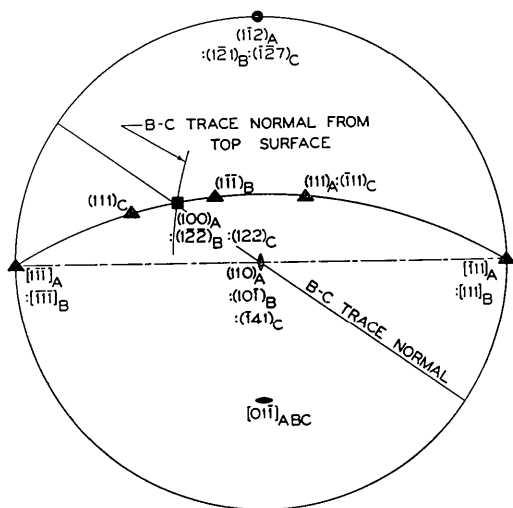


Fig. 5. Composite stereographic projection of twin components in silicon bar of Fig. 3. The front surface lies in the plane of projection with the longitudinal axis horizontal.

Table I. Surfaces of twinned components

Component	A	B	C
Front surface	(110)	(10 $\bar{1}$)	($\bar{1}41$)
Top surface	($\bar{1}\bar{1}2$)	($\bar{1}2\bar{1}$)	($\bar{1}27$)
Growth direction	[$\bar{1}11$]	[111]	[511]

sists of $(\bar{1}22)_B = (122)_C$, a form of second-order twin boundary which can be shown to be coherent in the diamond structure by the coincidence site superlattice constructed after Ellis & Treuting (1951). This second-order boundary has been described by Whitwham, Mouflard & Lacombe, 1951.

It is immediately evident that the surface contour traces are consistent with the development of $\{111\}$ planes as the pit walls. It is not at once evident that the developed planes are exclusively of the $\{111\}$ form and not, for example, any plane of the $\langle 110 \rangle$ zone. To fix this, one reasonable assumption must be introduced: that only one form of crystal plane is in fact developed in the pits. On this hypothesis pit traces on different surfaces may be paired, each pair representing the intersections on these surfaces of a single crystal plane. It is then found that on constructing the normals to the pit traces on the stereographic projection in the plane of the front surface, and on rotating trace normals on the top surface into this same projection plane, the sets of normals intersect in pairs at the $\{111\}$ poles. Thus the crystal planes

bounding the pits are shown to be $\{111\}$ planes in all cases.

Concluding remarks

It is easy to initiate melting by the electrical method described above without danger of melting the entire crystal because of the extremely large heat of fusion of silicon. More heat is required to fuse the crystal than to raise it from room temperature to its melting point. In order to determine the temperature at which melt patterns begin to form, some experiments using an electric furnace were carried out in cooperation with C. D. Thurmond. Heating for 15 min. at 1395°C . produced no patterns but a like treatment at 1400°C . (12°C . below the melting point) gave random melt patterns. We believe that impurities on the surface lower the melting point in their immediate vicinity sufficiently to initiate localized melting and thus produce the phenomenon described here. This view was verified by deliberately plating metal impurities on the surface and producing melt patterns at predetermined locations. It was shown experimentally that melt patterns do not tend to form at crystal imperfections such as edge dislocations subsequently revealed by etching.

We have generated surface melt patterns of the same form as those on silicon on a number of other materials having a diamond-like structure. These include germanium, indium antimonide, gallium antimonide, and gallium arsenide. (Preliminary studies on indium antimonide by Millea & Tomizuka (1956) disclosed melt patterns apparently bounded by $\{111\}$ planes.) Electric heating methods similar to those described above were used, excepting that an inert atmosphere was required to eliminate surface oxidation.

We wish to thank W. C. Ellis for his helpful discussions, E. E. Thomas for preparing the photomicrographs, and W. L. Feldmann for aid in the experimental work.

References

- BARRETT, C. S. (1952). *Structure of Metals*, 2nd ed., p. 39. New York: McGraw-Hill.
- BOND, W. L. (1946). *Amer. Min.* **31**, 31.
- BOND, W. L. (1948). *Amer. Min.* **33**, 703.
- BOND, W. L. & LOGAN, R. A. (1958). To be published.
- ELLIS, W. C. & TREUTING, R. G. (1951). *Amer. Inst. Min. (Metall.) Engrs.* **191**, 53.
- MILLEA, M. F. & TOMIZUKA, C. Z. (1956). *J. Appl. Phys.* **27**, 96.
- OLETE, M. (1957). *C. R. Acad. Sci., Paris*, **244**, 1033.
- STRAUMANIS, M. E. & AKA, E. J. (1952). *J. Appl. Phys.* **23**, 330.
- WHITWHAM, D., MOUFLARD, M. & LACOMBE, P. (1951). *Amer. Inst. Min. (Metall.) Engrs.* **191**, 1070.